Astron. Astrophys. 342, 192–200 (1999)

ASTRONOMY AND ASTROPHYSICS

Direct Urca process in strong magnetic fields and neutron star cooling

D.A. Baiko and D.G. Yakovlev

A.F. Ioffe Physical Technical Institute, Politekhnicheskaya 26, 194021 St.Petersburg, Russia

Received 14 August 1998 / Accepted 3 November 1998

Abstract. The effect of the magnetic field on the energy loss rate in the direct Urca reactions is studied. The general expression for the neutrino emissivity at arbitrary magnetic field B is derived. The main emphasis is laid on a case, in which the field is not superstrong, and charged reacting particles (e and p) populate many Landau levels. The magnetic field keeps the process operative if $\Delta k/k_{Fn} \lesssim N_{Fp}^{-2/3}$ (N_{Fp} is the number of the Landau levels populated by protons and $\Delta k \equiv k_{Fn} - k_{Fp} - k_{Fe}$), that is beyond the well–known switch–on limit in the absence of the field, $\Delta k < 0$. Cooling of magnetized neutron stars with strong neutron superfluid in the outer cores and nonsuperfluid inner cores is simulated. The magnetic field near the stellar center speeds up the cooling if the stellar mass M is slightly less than the minimum mass M_c, at which the direct Urca reaction becomes allowed for $B = 0$. If $B = 3 \cdot 10^{16}$ G, the affected mass range is $M_c - M \lesssim 0.1\, M_c$, while for $B = 3 \cdot 10^{15}$ G the range is $M_c - M \lesssim 0.015\, M_c$. This may influence a theoretical interpretation of the observed thermal radiation as illustrated for the Geminga pulsar. The case of superstrong magnetic fields ($B \gtrsim 10^{18}$ G), such that e and p populate only the lowest Landau levels is briefly outlined.

Key words: nuclear reactions, nucleosynthesis, abundances – stars: neutron – pulsars: individual: Geminga = 1E 0630+1

1. Introduction

The presence or absence of the direct Urca process ($n \to e + p + \bar{\nu}_e$, $e + p \to n + \nu_e$) in the core of a neutron star is the most important issue of the stellar cooling. If operative, it dominates the cooling at the neutrino stage (age $t \lesssim 10^5$ – 10^6 yr) being several orders of magnitude more efficient than any other neutrino emission process (e.g., Pethick, 1992). However, the direct Urca can occur under stringent conditions: one requires quite high fraction of protons [$k_{Fn} \leq k_{Fp} + k_{Fe}$, where $k_{F\alpha} = (3\pi^2 n_\alpha)^{1/3}$ is a Fermi momentum, and n_α is a number density of particles of species α] in order to conserve momentum in the reaction. Nevertheless, some equations of state (EOSs) allow for that (Lattimer et al., 1991). On the other hand, most realistic EOS of dense matter (Wiringa et al., 1988) predicts too small fraction of protons, which decreases with growing density; consequently, the direct Urca is forbidden in the entire neutron star core.

In this paper we study the possibility for the direct Urca to be open in the presence of a magnetic field B, if the proton fraction is too low to open the process at $B = 0$. The beta–decay and related reactions in strong magnetic fields have been studied since late 1960's (e.g., Canuto & Chiu 1971, Dorofeev et al. 1985, Lai & Shapiro 1991, and references therein). However, these results have been obtained under various simplified assumptions (constant matrix elements, non–degenerate nucleons, etc.) and do not give the emissivity of the direct Urca reaction in the neutron star cores. Several works on the subject have appeared most recently. Leinson & Pérez (1997) considered the case of superstrong fields ($B \gtrsim 10^{18}$ G), in which electrons and protons occupy only the lowest Landau levels. They found that such fields relaxed the requirement of high proton fraction, and the direct Urca was always permitted leading to a rapid cooling of a neutron star. The case of superstrong fields was examined also by Bandyopadhyay et al. (1998). These authors found, by contrast, that the condition "$k_{Fn} \leq k_{Fp} + k_{Fe}$" (quotation implies that one should be careful with definition of the Fermi momentum in superstrong fields) still determined the direct Urca threshold, and that the fields enhanced the neutrino emissivity by 1 – 2 orders of magnitude in the permitted regime compared to the standard value (Lattimer et al., 1991)

$$Q_\nu^0 = 4 \cdot 10^{27} (n_e/n_0)^{1/3}\, T_9^6\, \frac{m_n^* m_p^*}{m_n m_p} \text{ erg cm}^{-3} \text{ s}^{-1} . \tag{1}$$

Here $T_9 = T/10^9$ K, n_e is the electron density, $n_0 = 0.16\,\text{fm}^{-3}$, m_n^* and m_p^* are nucleon effective masses in dense matter, m_n and m_p are their bare masses.

The present paper is organized as follows.

In Sect. 2 we obtain a general expression for the neutrino emissivity Q_ν of the direct Urca process.

In Sect. 3 we concentrate on a realistic case, in which the magnetic field is not extremely high (although still high: $B \leq 3 \cdot 10^{16}$), and charged particles populate many Landau levels. We show that the field keeps the direct Urca open slightly outside the region where $k_{Fn} < k_{Fp} + k_{Fe}$ (the standard, $B = 0$, definition of k_F applies).

In Sect. 4 we illustrate this result by a series of cooling simulations of magnetized neutron stars with no superfluid in the inner cores and neutron superfluid in the outer cores.

Finally, in Sect. 5 we treat briefly the case of super strong magnetic fields. We show that the results by Leinson & Pérez (1997) are basically correct, although not very accurate in details, while those reported by Bandyopadhyay et al. (1998) are inaccurate.

2. Quantum formalism

In this section we obtain a general formula for the neutrino energy emission rate in the direct Urca reactions valid at any magnetic field $B \ll 10^{20}$ G (at higher fields protons become relativistic). The calculation is done in the Born approximation within the standard quantum mechanical framework with weak interactions described by the Weinberg–Salam–Glashow theory. We adopt the conventional assumption that reacting electrons are relativistic, while protons and neutrons are nonrelativistic. All these particles are strongly degenerate. The rate of transition from an initial state $|i\rangle$ to a final state $|f\rangle$ is $Q_{fi} = 2\pi\hbar^{-1}V^{-1}|\langle f|\mathcal{H}|i\rangle|^2\delta(\mathcal{E}_f - \mathcal{E}_i)$, where V is the normalization volume and $\mathcal{H}$ describes weak interaction in the second–quantization formalism. For the neutron decay, we have ($c = \hbar = 1$)

$$\mathcal{H} = \frac{G}{\sqrt{2}} \int_{(V)} \mathrm{d}\mathbf{r}\; \hat{\psi}_p^\dagger(\delta_{\mu 0} - g_A\delta_{\mu i}\sigma_i)\hat{\psi}_n\, \hat{\bar{\psi}}_e\gamma^\mu(1+\gamma^5)\hat{\psi}_\nu. \quad (2)$$

In this case, $G = G_F\cos\theta_C$, $G_F = 1.436\cdot 10^{-49}$ erg cm^3 is the Fermi weak coupling constant, $\theta_C \approx 13^\circ$ is the Cabibbo angle, $g_A = 1.261$ is the axial–vector coupling constant, σ_i is a Pauli matrix, and γ^μ is a Dirac matrix. Finally, $\hat{\psi}_\alpha$ is a field operator in the coordinate representation, i.e., the expression of the form $\sum_q \hat{a}_q\psi_q(\mathbf{r})$, where q denotes full set of quantum numbers, $\hat{a}_q$ is an annihilation operator, and $\psi_q(\mathbf{r})$ is an eigenstate.

To evaluate the total neutrino energy loss rate (emissivity) we need to sum Q_{fi} times the energy of the newly born antineutrino over all initial and final states. First of all, we can sum the matrix element $|\langle f|\mathcal{H}|i\rangle|^2$ over the electron spin states. The energy–conserving delta–function is not affected by this summation, since all, except the lowest, electron states are spin–degenerate. Choosing the Landau gauge of the vector potential $\mathbf{A} = (-By, 0, 0)$ and performing a tedious calculation, we get

$$\sum_{\sigma_e} |\langle f|\mathcal{H}|i\rangle|^2 \;=\; \frac{(2\pi)^2 M}{L_x L_z V^2}\,\delta(k_{nz} - k_{ez} - k_{pz} - k_{\nu z}) \times\; \delta(k_{nx} - k_{ex} - k_{px} - k_{\nu x}), \quad (3)$$

where

$$\begin{aligned}\frac{M}{G^2} \;=\;& \frac{1}{2}\,\delta_{s_p s_n}\,(1+g_A^2)\left[\left(1-\frac{k_{ez}}{\varepsilon_e}\right)\left(1-\frac{k_{\nu z}}{\varepsilon_\nu}\right)F'^2 + \left(1+\frac{k_{ez}}{\varepsilon_e}\right)\left(1+\frac{k_{\nu z}}{\varepsilon_\nu}\right)F^2\right] \\ &+ \delta_{s_p s_n}\,g_A\,s_p\left[\left(1-\frac{k_{ez}}{\varepsilon_e}\right)\left(1-\frac{k_{\nu z}}{\varepsilon_\nu}\right)F'^2 - \left(1+\frac{k_{ez}}{\varepsilon_e}\right)\left(1+\frac{k_{\nu z}}{\varepsilon_\nu}\right)F^2\right] \\ &+ 2\,\delta_{s_p,1}\,\delta_{s_n,-1}\,g_A^2\left(1+\frac{k_{ez}}{\varepsilon_e}\right)\left(1-\frac{k_{\nu z}}{\varepsilon_\nu}\right)F^2 \\ &+ 2\,\delta_{s_p,-1}\,\delta_{s_n,1}\,g_A^2\left(1-\frac{k_{ez}}{\varepsilon_e}\right)\left(1+\frac{k_{\nu z}}{\varepsilon_\nu}\right)F'^2 \\ &+ \delta_{s_p s_n}\,(1-g_A^2)\frac{k_{e\perp}}{\varepsilon_e}\frac{\mathbf{k}_\nu\mathbf{q}}{\varepsilon_\nu q}\,FF'. \end{aligned} \quad (4)$$

In these equations, $k_{\alpha i}$ is a cartesian component of a particle momentum, ε_α is a particle energy, $s_p = \pm 1$ and $s_n = \pm 1$ are, respectively, the doubled proton and neutron spin projections onto the magnetic field direction, $k_{e\perp} = \sqrt{2bn}$, n is the electron Landau level number, $b \equiv |e|B$, $\mathbf{k}_\nu$ is the antineutrino wave vector, and $\mathbf{q} = (k_{nx} - k_{\nu x}, k_{ny} - k_{\nu y}, 0)$. L_x and L_z are the normalization lengths. Finally, $F = F_{n',n}(u)$ and $F' = F_{n',n-1}(u)$ are the Laguerre functions (e.g., Kaminker & Yakovlev, 1981), n' is the proton Landau level number, and $u = q^2/(2b)$. If any index (n or n') is negative, $F_{n,n'}(u) = 0$.

The next step consists in integrating over the x components of proton and electron momenta, which specify the y coordinates of the Larmor guiding centers of these particles. This operation gives the factor $L_x^2 L_y b/(2\pi)^2$ and removes the second delta–function in Eq. (3). Thus, we may write a general formula for the neutrino emissivity (including the inverse reaction which doubles the emission rate) as

$$\begin{aligned}Q_\nu \;=\;& \frac{2b}{(2\pi)^7}\sum_{nn's_ps_n}\int \mathrm{d}\mathbf{k}_n\,\mathrm{d}\mathbf{k}_\nu\,\mathrm{d}k_{pz}\,\mathrm{d}k_{ez} \\ &\times\; f_n\,(1-f_p)\,(1-f_e)\,\delta(\varepsilon_n - \varepsilon_e - \varepsilon_p - \varepsilon_\nu)\,\varepsilon_\nu \\ &\times\; \delta(k_{nz} - k_{ez} - k_{pz} - k_{\nu z})\,M. \end{aligned} \quad (5)$$

In this case, $f_\alpha = (1+\exp\left[(\varepsilon_\alpha - \mu_\alpha)/T\right])^{-1}$ is a Fermi–Dirac distribution, and the particle energies are given by the familiar expressions:

$$\begin{aligned}\varepsilon_e \;&=\; \sqrt{m_e^2 + k_{ez}^2 + 2bn}, \\ \varepsilon_p \;&=\; \frac{k_{pz}^2}{2m_p^*} + \left[n' + \frac{1}{2}\left(1 - g_p s_p\frac{m_p^*}{m_p}\right)\right]\frac{b}{m_p^*}, \\ \varepsilon_n \;&=\; \frac{k_n^2}{2m_n^*} - \frac{g_n s_n b}{2m_p}, \qquad \varepsilon_\nu = k_\nu, \end{aligned} \quad (6)$$

with the proton and neutron gyromagnetic factors $g_p = 2.79$ and $g_n = -1.91$. In principle, the factors g_A, g_p, g_n can be renormalized in dense matter which we ignore, for simplicity.

Since the electron and proton distributions are independent of signs of k_{ez} and k_{pz} we can simplify the expression for M by omitting the terms which would anyway yield zero after the integration:

$$\begin{aligned}\frac{M}{G^2} \;=\;& \frac{1}{2}\,\delta_{s_p s_n}\,(1+g_A^2)\left[\left(1+\frac{k_{ez}}{\varepsilon_e}\frac{k_{\nu z}}{\varepsilon_\nu}\right)F'^2 + \left(1+\frac{k_{ez}}{\varepsilon_e}\frac{k_{\nu z}}{\varepsilon_\nu}\right)F^2\right] \\ &+ \delta_{s_p s_n}\,g_A\,s_p\left[\left(1+\frac{k_{ez}}{\varepsilon_e}\frac{k_{\nu z}}{\varepsilon_\nu}\right)F'^2\right.\end{aligned}$$

$$- \left(1+\frac{k_{ez}}{\varepsilon_e}\frac{k_{\nu z}}{\varepsilon_\nu}\right) F^2\Bigg]$$
$$+\ 2\ \delta_{s_p,1}\,\delta_{s_n,-1}\,g_A^2\ \left(1-\frac{k_{ez}}{\varepsilon_e}\frac{k_{\nu z}}{\varepsilon_\nu}\right) F^2$$
$$+\ 2\ \delta_{s_p,-1}\,\delta_{s_n,1}\,g_A^2\ \left(1-\frac{k_{ez}}{\varepsilon_e}\frac{k_{\nu z}}{\varepsilon_\nu}\right) F'^2$$
$$+\ \delta_{s_p s_n}\,(1-g_A^2)\,\frac{k_{e\perp}}{\varepsilon_e}\,\frac{\mathbf{k}_\nu \mathbf{q}}{\varepsilon_\nu q}\,FF'. \tag{7}$$

Keeping $k_{\nu z}$ in the z component of the momentum conserving delta–function in Eq. (5) would lead to a subtle thermal effect: it would mollify the resulting functions on a temperature scale. We will not pursue the accurate description of the effect here, both because the calculation would be quite complex, and because the temperature scale is assumed to be small. Therefore, we will neglect the neutrino momentum in the delta–function and, for the same reason, omit it from the definition of the vector **q**. Then, using the isotropy of the neutron distribution, we can further simplify the expression for M:

$$\frac{M}{G^2} \ =\ 2g_A^2\,\left(\delta_{s_p,1}\,\delta_{s_n,-1}\,F^2+\delta_{s_p,-1}\,\delta_{s_n,1}\,F'^2\right)$$
$$+\ \frac{1}{2}\ \delta_{s_p s_n}\,(1+g_A^2)\,\left(F'^2+F^2\right)$$
$$+\ \delta_{s_p s_n}\,g_A\,s_p\,\left(F'^2-F^2\right), \tag{8}$$

where the functions F and F' depend now on $u = (k_{nx}^2+k_{ny}^2)/(2b) \equiv k_{n\perp}^2/(2b)$.

Notice that the results of this and subsequent sections are equally valid for direct Urca processes involving hyperons. The results for hyperons are easily obtained by changing the values of reaction constants (g_A, etc.) as described, for instance, by Prakash et al. (1992).

3. Quasiclassical case

(a) General treatment and limit $B \to 0$. First of all consider the most realistic case of not too high magnetic fields, in which electrons and protons populate many Landau levels. In this case the transverse wavelengths of electrons and protons are much smaller than their Larmor radii. Thus the situation may be referred to as quasiclassical, and corresponding techniques apply. If the main contribution comes from large n and n', the difference between F^2 and F'^2 can be neglected. Moreover, we can neglect the contributions of magnetic momenta of particles to their energies. Thus, we can pull all the functions of energy out of the sum over s_n and s_p, and evaluate the latter sum explicitly:

$$\sum_{s_n s_p} M = 2\,G^2\,(1+3g_A^2)\,F^2. \tag{9}$$

Inserting this into Eq. (5), and integrating over orientations of neutrino momentum we get

$$Q_\nu \ =\ \frac{16\pi G^2\,(1+3g_A^2)\,b}{(2\pi)^7}\int \mathrm{d}\varepsilon_\nu\,\mathrm{d}\mathbf{k}_n\,\mathrm{d}k_{pz}\,\mathrm{d}k_{ez}\,\varepsilon_\nu^3$$
$$\times\ \sum_{nn'} F_{n',n}^2(u)\,f_n\,(1-f_p)\,(1-f_e)$$
$$\times\ \delta(\varepsilon_n-\varepsilon_e-\varepsilon_p-\varepsilon_\nu)\,\delta(k_{nz}-k_{ez}-k_{pz}), \tag{10}$$

where

$$\varepsilon_p = \frac{k_{pz}^2+k_{p\perp}^2}{2m_p^*}, \quad \varepsilon_n = \frac{k_n^2}{2m_n^*}, \tag{11}$$

$k_{p\perp} = \sqrt{2bn'}$, while the electron energy is still given by Eq. (6).

If the magnetic field is not too large the transverse electron and proton momenta, $k_{e\perp}^2$ and $k_{p\perp}^2$, are sampled over a dense grid of values, corresponding to integer indices n and n'. Thus, the double sum in Eq. (10) tends to the double integral over $k_{e\perp}^2$ and $k_{p\perp}^2$,

$$2b\sum_{nn'} F_{n',n}^2(u)\ldots \to \int \mathrm{d}k_{e\perp}^2\mathrm{d}k_{p\perp}^2\ \mathcal{F}\ldots, \tag{12}$$

where $\mathcal{F}$ represents the small–b asymptote of the function

$$\frac{1}{2b}F_{Np,Ne}^2(u)\,, \tag{13}$$

with $N_p \equiv k_{p\perp}^2/(2b)$ and $N_e \equiv k_{e\perp}^2/(2b)$.

After replacing the double sum by the double integral Eq. (10) can be considerably simplified. Note, that $\mathrm{d}k_z\,\mathrm{d}k_\perp^2 = \mathrm{d}\mathbf{k}/\pi = 2m^*\,\mathrm{d}\varepsilon\,k\,\sin\theta\,\mathrm{d}\theta$, where θ is a pitch–angle. Then the energy integral $\int \mathrm{d}\varepsilon_n\,\mathrm{d}\varepsilon_p\,\mathrm{d}\varepsilon_e\,\mathrm{d}\varepsilon_\nu$ is taken by assuming, that the temperature scale is small and provides the sharpest variations of the integrand. If so, we can set $k = k_F = (3\pi^2 n)^{1/3}$, $\varepsilon = \varepsilon_F$ etc. in all the other functions. In principle, this assumption constraints the validity of the quasiclassical approach. We will come back to this point at the end of this section. Finally, we integrate over the azimuthal angle of the neutron momentum, and over its polar angle to eliminate the momentum conserving delta–function, and obtain:

$$Q_\nu \ =\ Q_\nu^0 \times R_B^{\rm qc};$$
$$Q_\nu^0 \ =\ \frac{457\pi\,G^2\,(1+3g_A^2)}{10080}\,m_n^*\,m_p^*\,\mu_e\,T^6,$$
$$R_B^{\rm qc} \ =\ 2\int\int_{-1}^{1}\mathrm{d}\cos\theta_p\,\mathrm{d}\cos\theta_e\,\frac{k_{Fp}k_{Fe}}{4b}\,F_{Np,Ne}^2(u)$$
$$\times\ \Theta(k_{Fn}-|k_{Fp}\cos\theta_p+k_{Fe}\cos\theta_e|), \tag{14}$$

where Q_ν^0 is the field–free emissivity (1), and the factor $R_B^{\rm qc}$ describes the effect of the magnetic field. $k_{p,e\perp} = k_{Fp,e}\sin\theta_{p,e}$, and $k_{n\perp}^2$ is now given by $k_{Fn}^2 - (k_{Fp}\cos\theta_p + k_{Fe}\cos\theta_e)^2$; $\Theta(x) = 1$ for $x > 0$, $\Theta(x) = 0$ for $x < 0$.

The asymptotic behaviour of (13) depends on the relation between the argument of the function F and its indices. In the small–b case one can distinguish three domains of these parameters: (I) $k_{n\perp} < |k_{p\perp} - k_{e\perp}|$; (II) $|k_{p\perp} - k_{e\perp}| < k_{n\perp} < (k_{p\perp} + k_{e\perp})$; and (III) $(k_{p\perp} + k_{e\perp}) < k_{n\perp}$. In domains (I) and (III) the asymptotes in question decay exponentially when $k_{n\perp}$ departs from the domain boundaries (which are the turning points of corresponding quasiclassical equation, e.g., Kaminker & Yakovlev, 1981). In both cases the exponents are inversely proportional to b, and both asymptotes tend to zero as $b \to 0$, although nonuniformly in the vicinities of the turning points. In domain (II), the asymptote of the expression (13) oscillates according to

$$\mathcal{F} \approx \frac{1}{\pi p b}\cos^2\Phi\,, \quad p = \sqrt{4N_pN_e - (N_p+N_e-u)^2}\,, \tag{15}$$

with a prefactor that is actually independent of b. The cosine phase is

$$\Phi = -(1+N_p)\arg(u+N_p-N_e,-ip) + N_e\arg(u+N_e-N_p,ip) - \frac{p-\alpha}{2}\,, \tag{16}$$
$$e^{i\alpha} = \frac{p(N_p-N_e)+i\left[(N_p-N_e)^2-u(N_p+N_e)\right]}{2u\sqrt{N_pN_e}}\,,$$

where $\arg(z)$ is an argument of complex number z which lies in the range $[-\pi,\pi]$. For integer indices, this formula coincides with Eq. (30) in Kaminker & Yakovlev (1981), and it provides an accurate extension of $\mathcal{F}$ to non–integer indices. One can easily show that a natural continuation of $F^2_{Np,Ne}(u)/(2b)$ to this case is given by the analytical function $W^2_{km}(u)/[2bu\Gamma(N_e+1)\Gamma(N_p+1)]$, where $W_{km}(u)$ is the Whittaker function, $u=k^2_{n\perp}/(2b)$, $k=(1+N_p+N_e)/2$, and $m=(N_e-N_p)/2$. Eqs. (15) and (16) are derived using accurate small–b asymptotes of $W_{km}(u)$, which, in turn, could be derived from the integral representation of this function by the saddle–point method.

This information is sufficient to check, if $R^{\rm qc}_B$ reproduces the well–known step–function $\Theta(k_{Fp}+k_{Fe}-k_{Fn})$ in the $b\to 0$ limit. If $k_{Fn}>k_{Fp}+k_{Fe}$, we are always in domain (III) (since the z-momentum is conserved), and $R^{\rm qc}_B\to 0$. If, on the contrary, $k_{Fn}<k_{Fp}+k_{Fe}$ the integration in (14) covers all three domains, and the boundary of domain (II) corresponds to vanishing square root in Eq. (15). The contribution from domains (I) and (III) is again zero, while the integration over domain (II) yields exactly 1. To verify this, one can put the rapidly oscillating $\cos^2\Phi$ equal to $1/2$ in Eq. (15), and change the integration variables: $s=\cos\theta_p+\cos\theta_e$, $t=\cos\theta_p-\cos\theta_e$. In all cases, theta–function in Eq. (14) plays no role.

(b) Effect of the magnetic field in the forbidden domain ($k_{Fn}>k_{Fp}+k_{Fe}$). In a finite magnetic field, the border between the open and closed direct Urca regimes is expected to be smeared out over some scale depending on the field strength. This can be important for neutron star cooling, since the direct Urca process can remain the dominant energy loss mechanism even if it is suppressed exponentially by several orders of magnitude.

To investigate this possibility, one has to calculate the emissivity Q_ν from Eq. (10). We have used two approaches, one of which is essentially quasiclassical and good for a rapid computation, while the other is of quantum nature — more precise and time–consuming.

At the moment it is convenient to introduce two parameters, x and y, which characterize the reaction kinematics with respect to the magnetic field strength:

$$x=\frac{k^2_{Fn}-(k_{Fp}+k_{Fe})^2}{k^2_{Fp}\,N_{Fp}^{-2/3}},\quad y={N_{Fp}}^{2/3}, \tag{17}$$

where $N_{Fp}=k^2_{Fp}/(2b)$ is the number of the Landau levels populated by protons. The most interesting situation, from practical point of view, occurs if x is positive and not very large (say $x\lesssim 10$), since whenever k_{Fn} significantly exceeds $k_{Fp}+k_{Fe}$, the reaction is suppressed too strongly. The first approach is based on Eq. (14). The main contribution to this integral comes from the vicinity of the line $\theta_p=\theta_e$, corresponding to the least distance from $k_{n\perp}$ to domain (II). Since this distance should not be large, we may use in (14) the small–b asymptotic form of (13) in the neighbourhood of the right turning point, i.e., for $k_{n\perp}\approx k_{p\perp}+k_{e\perp}$. It is given, for instance, by Kaminker & Yakovlev (1981) and reads

$$F^2_{Np,Ne}(u) \approx \frac{(2b)^{2/3}(k_{p\perp}k_{e\perp})^{-1/3}}{(k_{p\perp}+k_{e\perp})^{2/3}}\ {\rm Ai}^2(\xi) = \frac{(\sin\theta_p\sin\theta_e)^{-1/3}}{y\,(\sin\theta_p+\sin\theta_e)^{2/3}}\ {\rm Ai}^2(\xi), \tag{18}$$

$$\xi = \frac{\left[k^2_{n\perp}-(k_{p\perp}+k_{e\perp})^2\right](k_{p\perp}k_{e\perp})^{1/3}}{(2b)^{2/3}(k_{p\perp}+k_{e\perp})^{4/3}} \approx \left[x+2y\left(1-\cos\left(\theta_p-\theta_e\right)\right)\right]\frac{(\sin\theta_p\sin\theta_e)^{1/3}}{(\sin\theta_p+\sin\theta_e)^{4/3}},$$

where ${\rm Ai}(\xi)$ is the Airy function, defined as in Abramowitz & Stegun (1970), and we have assumed $k_{Fp}=k_{Fe}$, which implies absence of muons and hyperons in neutron–star matter. At negative arguments, which correspond to domain (II), the Airy function oscillates, while for positive arguments, in domain (III), it decreases exponentially approaching the asymptote

$${\rm Ai}^2(\xi)\approx\frac{1}{4\pi\sqrt{\xi}}\ \exp\left(-\frac{4}{3}\xi^{3/2}\right),\quad \xi\gg 1. \tag{19}$$

Inserting the latter equation into Eq. (14), we find, that at relatively large x

$$R^{\rm qc}_B\approx\sqrt{\frac{y}{x+12\,y}}\ \frac{3}{x^{3/2}}\ \exp\left(-\frac{x^{3/2}}{3}\right). \tag{20}$$

At very large x, however, this asymptote should not be taken too literally because Eq. (18) ceases to be valid far from the turning point.

On the other hand, under quasiclassical assumptions, we are always interested in the case of $y\gg 1$. If so, we can further simplify Eq. (14) at any x using (18), and noting that all the functions can be expanded around the line $\theta_p=\theta_e$. Then we obtain

$$R^{\rm qc}_B = 2^{-2/3}\int_{-\infty}^{\infty}{\rm d}s\int_0^{\pi}{\rm d}\theta\ \sin^{2/3}\theta\ {\rm Ai}^2(\xi), \tag{21}$$
$$\xi = \frac{x+s^2}{2^{4/3}\sin^{2/3}\theta}.$$

At $x=0$ this integral is taken analytically and gives $R^{\rm qc}_B=1/3$. By inserting Eq. (19), one easily verifies, that Eq. (21) reproduces also the asymptote (20) for $x\ll 12y$.

Finally, we have calculated the factor $R^{\rm qc}_B$, using both prescriptions (14) + (18), and (21) at $N_{Fp}\equiv y^{3/2}=100,\ 1000,\ 10000$ and x from 0 to 20. In both these cases we have obtained identical results. This indicates that for such combinations of x and y, the y–dependence of $R^{\rm qc}_B$ is insignificant.

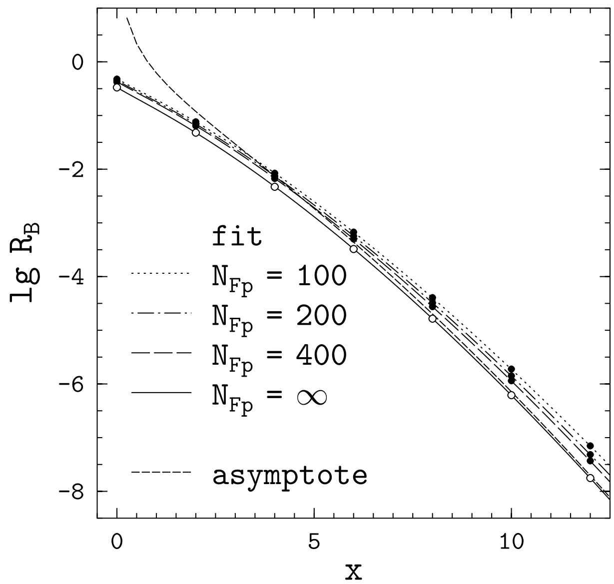

Fig. 1. Logarithm of R_B as a function of x in the forbidden domain $\Delta k \equiv k_{Fn} - k_{Fp} - k_{Fe} > 0$ for various values of N_{Fp}. Open circles correspond to the quasiclassical approach ($R_B^{\rm qc}$), insensitive to the value of N_{Fp}, while solid circles show the quantum numerical results. The short–dash line is the asymptote (20). Other curves are calculated from the fitting formula (22).

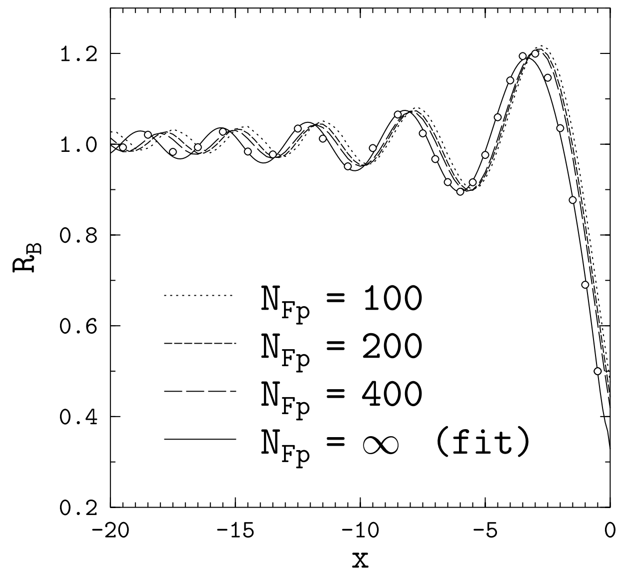

Fig. 2. Factor R_B in the permitted domain $\Delta k < 0$ as a function of x for various values of N_{Fp}. Open circles correspond to the quasiclassical approach (21), solid line is calculated from the fitting formula (23), and the other curves represent the quantum numerical results.

These results are plotted in Fig. 1 by open circles. The short–dashed curve represents the asymptote (20).

In the quasiclassical approach we have made two approximations: firstly, we have replaced the sum by the integral at finite b, and, secondly, we substituted the asymptote in the form of the Airy function for the function F. To assess the quality of both assumptions we have used a quantum approach based directly on Eq. (10).

In this approach, if one transforms the integration over k_z to that over ε in a straightforward manner, the integrand becomes singular (the denominators of the form $\sqrt{\varepsilon - \varepsilon_n}$ appear). If $T \to 0$ the quantity Q_ν/T^6 diverges at integer N_{Fp}. For nonzero T this quantity remains convergent but oscillates as a function of B and/or density. These oscillations are quite familiar and appear in many studies (magnetization, electrical and thermal conductivities, etc., Landau and Lifshitz, 1986). They are associated with population of the Landau levels by electrons and protons due to variation of plasma parameters.

If T is larger than the energy spacing between the Landau levels the oscillations are washed out, and a smooth curve emerges. This regime requires very accurate integration over particle momenta in order to include thermal effect. We were able to perform it only for rather small $N_{Fp} \lesssim 20$ and do not report these results here. In a more important case of lower temperatures the summation over Landau levels and energy integration are independent. The actual neutrino emissivity does oscillate but the quantity of practical significance is the emissivity averaged over the oscillations (a smooth curve again). We call this approach quantum since it involves the summation over Landau levels explicitly. In this way we have calculated the emissivity and smoothed the oscillations artificially by two different methods. We have checked that both methods yield nearly identical smoothed Q_ν. Simple consideration (see the end of this section) shows that this (nonthermal quantum) approach is valid for $T < \sqrt[3]{N_{Fp}}\omega_B$, or, equivalently, $N_{Fp}^{2/3} < \mu_p/T$, where ω_B is the proton gyrofrequency and μ_p is the proton chemical potential.

The results of these calculations are presented in Fig. 1 for $N_{Fp} = 100,\ 200$, and 400 by solid circles. It is seen that with increasing N_{Fp} the quantum factor R_B tends to the quasiclassical one $R_B^{\rm qc}$.

We have also found the fit expression that describes accurately (Fig. 1) the quantum calculations for $0 \le x \le 20$ and $N_{Fp} \ge 100$ and reproduces the quasiclassical curve in the limit $N_{Fp} \to \infty$:

$$\begin{aligned} R_B &= \frac{(3x + 6.800)\,R}{(x_c + 6.800)(3 + x\sqrt{12})}\,\exp\left(-\frac{x_c}{3}\right), \qquad (22)\\ R &= P_1 + P_2 {\rm e}^{P_3 x} + P_4 x, \\ P_1 &= 1 + \frac{3.801}{N_{Fp}^{0.5280}}, \quad P_2 = 1 + \frac{2.242}{N_{Fp}^{0.3498}} - P_1, \\ P_3 &= 0.07221 + \frac{1.751}{N_{Fp}^{0.5001}}, \quad P_4 = \frac{1.551}{N_{Fp}^{0.8128}}, \\ x_c &= x\,\sqrt{x + 0.4176} - 0.04035\,x. \end{aligned}$$

(c) Effect of the magnetic field in the permitted domain ($k_{Fn} < k_{Fp} + k_{Fe}$). Since $R_B < 1$ at $x = 0$, one may expect that the magnetic field has a non–trivial effect on the neutrino emissivity in the permitted domain. This appears to be true. Applying the quasiclassical approach in the form of Eq. (21) at negative x, we obtain for $R_B^{\rm qc}$ an oscillating curve, shown in Fig. 2 by the open circles. Using the more accurate quantum

approach we get a series of the curves for $N_{Fp} = 100,\ 200$, and 400, the curve with highest N_{Fp} being again the closest to the quasiclassical result. These oscillations are of quasiclassical nature and have nothing in common with the quantum oscillations discussed above. From the practical point of view, they are not very important, as they hardly have any noticeable effect on the neutron star cooling. Note, that the results for $-20 \leq x \leq 0$ and $N_{Fp} = \infty$ are accurately fitted by the expression (solid curve in Fig. 2)

$$R_B = 1 - \frac{\cos\varphi}{(0.5816 + |x|)^{1.192}}, \qquad (23)$$
$$\varphi = \frac{1.211 + 0.4823|x| + 0.8453|x|^{2.533}}{1 + 1.438|x|^{1.209}}.$$

To summarize, we remind that the direct Urca reaction in the $B = 0$ case is operative if the momentum excess $\Delta k \equiv k_{Fn} - k_{Fp} - k_{Fe} < 0$. In the presence of the magnetic field, the condition becomes less stringent, and the reaction becomes quite efficient as long as $x \lesssim 10$, i.e., $\Delta k / k_{Fn} \lesssim N_{Fp}^{-2/3}$. If, for instance, $B = 10^{16}$ G, and the density of matter is near the direct Urca threshold, one typically has $N_{Fp} \sim 300$ and $\Delta k / k_{Fp} \lesssim 1/25$.

Notice that the field–free direct Urca process can also be allowed beyond the domain $\Delta k < 0$ due to the $thermal$ smearing of the Fermi surface. If $B = 0$ and $\Delta k > 0$ the reaction rate can be written as $Q_\nu = Q_\nu^0 \times R_T$, where R_T may be expected to be $\propto \exp(-v_{Fp}\,\Delta k / T)$. Thus the thermal effect extends the reaction to the domain where $\Delta k / k_{Fp} \lesssim T/\mu_p$. The smearing is clearly determined by the proton degeneracy parameter, μ_p/T, which is typically about 300 for $T \sim 10^9$ K. The magnetic field effect is more important than the thermal effect if $N_{Fp}^{2/3} \lesssim \mu_p/T$ that can often be the case in the inner cores of neutron stars.

4. Cooling of magnetized neutron stars

In this section we illustrate the above results by cooling simulations. Let us consider a set of neutron star models with fixed equation of state but varying central density and magnetic field strength. Specifically, we take the EOS by Prakash et al. (1988) with the compression modulus $K_0 = 180$ MeV and the symmetry energy in the form suggested by Page & Applegate (1992). It is assumed that matter in the stellar core consist of neutrons, protons and electrons (no muons and hyperons). The EOS predicts the monotonous increase of the proton fraction with increasing mass density. Therefore, if the central density ρ_c is higher than the certain threshold density $\rho_{\rm crit}$ (corresponding to proton fraction $x_p = n_p/n_b = 1/9$), or, equivalently, the stellar mass M is higher than the certain threshold mass M_c the direct Urca process becomes allowed in a central kernel of the inner stellar core. For the chosen EOS, the threshold parameters are $\rho_{\rm crit} = 12.976 \cdot 10^{14}$ g cm^{-3} and $M_c = 1.442 M_\odot$.

As pointed out by Page and Applegate (1992) the cooling history of a neutron star in the field–free regime is extremely sensitive to the stellar mass: if the mass exceeds M_c the star cools rapidly via the direct Urca process, while the cooling of the low–mass star is mainly due to the modified Urca process, and, therefore, is strongly delayed. The effect of the magnetic field would be to speed up the cooling of the star with a mass below M_c, because the strong field opens the direct Urca process even if the $B = 0$ condition $k_{Fn} \leq k_{Fp} + k_{Fe}$ (or $x_p \geq 1/9$) is not reached.

The magnetic field in the neutron star core may evolve on cooling time–scales. This may happen if the electric currents supporting the field are located in those regions of the core, where protons as well as neutrons are nonsuperfluid. If so, the electric currents transverse to the field may suffer enhanced ohmic decay due to magnetization of charged particles (e.g., Haensel et al., 1990). The consequences of the decay would be twofold. Firstly, if the strong field occupies a sufficiently large volume of the core, the decay produces an additional heating, which would delay the stellar cooling. Secondly, the field decay would reduce the direct Urca losses in the forbidden domain decreasing the factor R_B. If, however, the neutrons are strongly superfluid, the enhanced decay is absent (Haensel et al., 1990; Østgaard & Yakovlev, 1992), and the ohmic decay time of the internal magnetic field is typically larger than the Universe age (Baym et al., 1969).

On the other hand, microscopic calculations of superfluid neutron gaps in the neutron star core suggest that the critical temperatures are rather high at not too large densities (say, below 10^{15} g cm^{-3}), but decrease at higher densities (see, e.g., Takatsuka & Tamagaki, 1997, and references therein). Thus the electric currents could persist in the outer stellar core, where the neutron superfluid is available, and the enhanced field–decay mechanism does not work, while the direct Urca reactions operate in the inner core and are not subject to superfluid reduction. This latter scenario we adopt. We assume the presence of the magnetic field B in the stellar kernel, where the direct Urca process can be allowed, and assume nonsuperfluid protons in the neutron star core. Thus, the entire core is nonsuperconducting, and the magnetic field does not vary over the cooling time (age $t \lesssim 10^7$ yr) being frozen into the outer core.

Let us analyse the cooling stage at which the neutron star interior is isothermal ($t \gtrsim 10^2$ – 10^3 yr). The surface temperature T_s (seen by a distant observer, i.e., the gravitational redshift included) is then determined by the heat transport through the neutron star crust and is related uniquely to the internal temperature. We will use the cooling code described, for instance, by Levenfish & Yakovlev (1996), and Yakovlev et al. (1998). The effects of General Relativity are included explicitly. The neutrino luminosity is produced by the standard neutrino reactions in the entire stellar core complemented by the direct Urca process in the inner core. The effects of the neutron superfluidity on the neutrino reactions and neutron heat capacity in the outer core are taken into account as prescribed by Levenfish & Yakovlev (1996). In addition, we include the neutrino emission due to triplet–state Cooper pairing of neutrons (Yakovlev et al., 1998). The dependence of the surface temperature on the internal stellar temperature is taken from Potekhin et al. (1997) assuming no envelope of light elements at the stellar surface. To emphasize the effect of the internal magnetic fields on the neutron star cooling we neglect the presence of the surface mag-

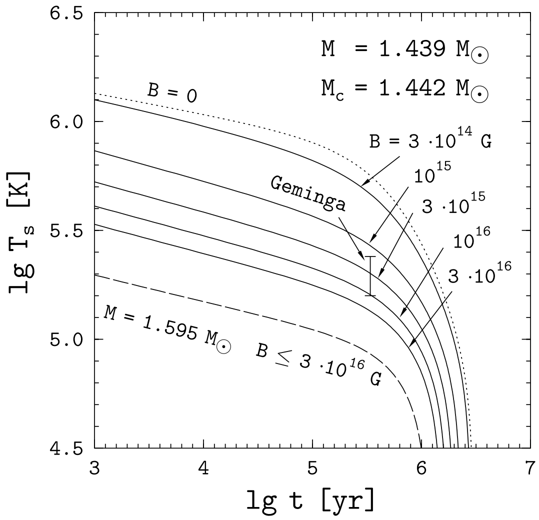

Fig. 3. Logarithm of the surface temperature as seen by a distant observer as a function of neutron star age. The dash curve is for a star of mass $M = 1.595 M_\odot$, well above the threshold mass M_c, with magnetic field $0 \leq B \leq 3 \cdot 10^{16}$ G. The dotted and solid curves are for the $1.439 M_\odot$ star. Bar shows observations of the Geminga pulsar (Meyer et al., 1994).

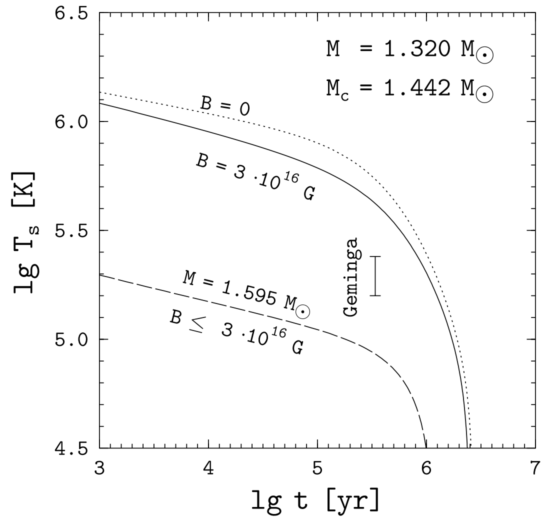

Fig. 4. Same as in Fig. 3. The dotted and solid curves are for the $1.320 M_\odot$ star. The dash line is the same as in Fig. 3.

netic fields and assume that the inner field does not affect the relationship between the surface and internal temperatures.

The density dependence of the neutron critical temperature (triplet–pairing) is given by the step–function: $T_{cn} = 10^{10}$ K at $\rho < 7.5 \cdot 10^{14}$ g cm^{-3}, and $T_{cn} = 0$ at $\rho \geq 7.5 \cdot 10^{14}$ g cm^{-3} The resulting cooling curves, $T_s(t)$, are insensitive to the initial inner temperature provided the latter is sufficiently high ($\gtrsim 10^9$K).

The cooling curves are depicted in Figs. 3 and 4. Dash line illustrates fast cooling due to direct Urca process allowed in a large portion of the core at $B = 0$. While calculating this curve we have used exact factors R_B in all the neutron–star layers where the field–free direct Urca is either permitted or forbidden. We have verified that the results are insensitive to specific values of R_B in the permitted domain. In that domain, one can safely use the quasiclassical fit (23) or even set $R_B = 1$. On the other hand, even a huge internal field is unimportant in the forbidden domain (the curves for $B = 0$ and $3 \cdot 10^{16}$ G coincide): new regions of the core, where the direct Urca is open by the field, amount for a negligible fraction of the total neutrino luminosity.

The upper dotted curves are calculated for the stars with masses 1.439 $M_\odot$ (Fig. 3) and 1.320 $M_\odot$ (Fig. 4) at $B = 0$. They represent the slow cooling via the standard neutrino reactions (the direct Urca is forbidden). The solid curves illustrate the effect of the magnetic field for the stars of the same masses. If the stellar mass is slightly (by 0.2%) below M_c (Fig. 3) the cooling curve starts to deviate from the standard one for not too high fields, $B = 3 \cdot 10^{14}$ G. Stronger fields, 10^{15}–$3 \cdot 10^{15}$ G produce the cooling intermediate between the standard and rapid ones, while still higher fields $B \gtrsim 10^{16}$ G open the direct Urca in a large fraction of the inner stellar core and initiate a nearly fully enhanced cooling. If, however, the mass is by about 8% below the threshold one (Fig. 4), only a very strong field $B = 3 \cdot 10^{16}$ G could keep the direct Urca process slightly open to speed up the cooling.

The results indicate that the magnetic field in the very central stellar core can indeed enhance the cooling provided the stellar mass is close to the threshold mass M_c. If $B = 3 \cdot 10^{16}$ G, the effect is significant in a mass range $M - M_c \lesssim 0.1\, M_c$. For lower fields the range becomes smaller. If, for instance, $B = 3 \cdot 10^{15}$ G, the mass range becomes as narrow as $M - M_c \lesssim 0.015\, M_c$.

Our results can be used for interpretation of observational data. By way of illustration, consider observations of the thermal radiation from the Geminga pulsar. Meyer et al. (1994) fitted the observed spectrum by the set of hydrogen atmosphere models. These fits yield rather low non–redshifted effective surface temperature $T_{\rm eff}$ = (2 – 3)$\cdot 10^5$ K. Introducing the appropriate redshift factor $g = \sqrt{1 - R_g/R} \approx 0.8$ (R is the stellar radius and R_g is the gravitational radius) one gets redshifted surface temperature $\lg T_s$ [K] $= 5.29 \pm 0.09$ ($T_s = g\, T_{\rm eff}$). Adopting the dynamical Geminga's age $t = 3.4 \times 10^5$ yr we can place the Geminga's error bar in Figs. 3 and 4. Let us use our cooling model (with possible strong magnetic field B near the stellar center unrelated to the much weaker Geminga's surface magnetic field). If $B = 0$ Geminga is found between the lines of standard ($M \leq M_c$) and fast ($M > M_c$) cooling. It is clear that tuning the mass slightly above M_c we can force the cooling curve to cross the error bar. However, the mass range corresponding to the bar width (Fig. 5) would be tiny (about $0.003 M_\odot$), as the cooling rate is extremely sensitive to M in the domain just above M_c. The narrowness of the confidence mass range makes it fairly improbable that the Geminga's mass lies in this range. Accordingly the suggested interpretation of the Geminga's cooling is unlikely. The situation becomes strikingly different in the presence of the strong magnetic field. The field shifts the confidence range of M (faded area in Fig. 5) below M_c (cf. Fig. 3), where variation of T_s with M at a given t is

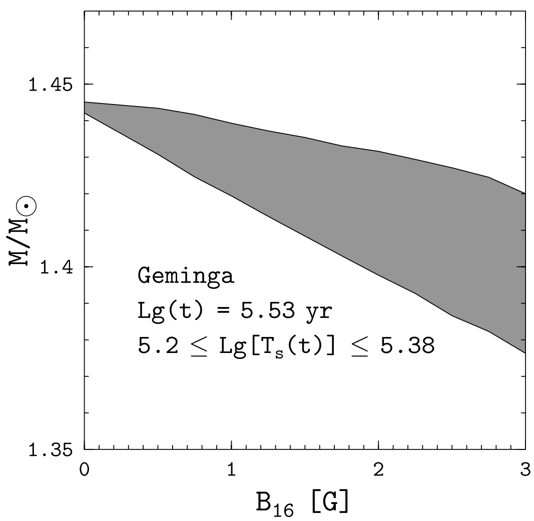

Fig. 5. The allowed mass range for the Geminga pulsar as a function of the internal magnetic field

much smoother. This widens considerably the confidence mass range. At $B = 10^{16}$ G it is about 0.02 $M_\odot$, while at $B = 3 \cdot 10^{16}$ G it is about 0.04 $M_\odot$ so that the chances that the Geminga's mass falls into this range become much higher. This makes the proposed interpretation more plausible.

5. The case of superstrong magnetic fields

Using the formalism of Sect. 2 let us outline the main features of the direct Urca reaction produced by electrons and protons occupying the lowest Landau levels (with proton spins aligned with the magnetic field). Notice, however, that one needs superhigh magnetic field, $B \gtrsim 10^{18}$ G, to force all electrons and protons into their ground Landau levels. Let n_e and n_p be the number densities of these particles. Contrary to the field–free Fermi momenta valid at not too high fields and used in Sects. 3 and 4, the limiting momenta along the superhigh magnetic field become field–dependent, $k^0_{e,p} = 2\pi^2 n_{e,p}/b$, $k^0_e \approx \mu_e$. The distribution of neutrons can be characterized by two Fermi momenta for particles with spins along and against the magnetic field k_{Fn,s_n}, $k_{Fn,1} < k_{Fn,-1}$. Our starting point is Eq. (8), which reduces to

$$M \;=\; G^2\, F^2 \left[\frac{1}{2}(1-g_A)^2\, \delta_{s_n,1} + 2g_A^2\, \delta_{s_n,-1}\right]. \qquad (24)$$

$$F^2 \;=\; F^2_{00} = \exp\left(-\frac{k^2_{n\perp}}{2b}\right).$$

Let us insert it into Eq. (5), neglect $k_{\nu z}$ in the momentum–conserving delta function, and integrate over the neutrino orientations and over an azimuthal angle of the neutron momentum. Then we convert the integrals over k_{ez} and k_{pz} into the integrals over particle energies, take the standard energy integral, and perform the integration over the neutron pitch–angle. We obtain (the inverse reaction included)

$$Q_\nu \;=\; \frac{457\pi\, G_F^2\,(1+3g_A^2)}{10080} m_n^* m_p^*\, \mu_e T^6$$
$$\times\; \frac{b}{k^0_p k^0_e\,(1+3g_A^2)} \sum_{\alpha=\pm1} \left[\frac{1}{4}\,(1-g_A)^2\,\Theta(u_{1\alpha})\, e^{-u_{1\alpha}}\right.$$
$$\left. +\; g_A^2\, \Theta(u_{-1\alpha})\, e^{-u_{-1\alpha}}\right], \qquad (25)$$

where $2b\, u_{s_n,\alpha} = k^2_{Fn,s_n} - (k^0_p + \alpha k^0_e)^2$, and $\alpha = \pm 1$ corresponds to two different reaction channels in which the electron and proton momenta along the z-axis are either parallel ($\alpha = 1$) or antiparallel ($\alpha = -1$). The step functions indicate that the channels are open if $u_{s_n,\alpha} \geq 0$. The channel $\alpha = -1$ is always open in npe dense matter with the superstrong magnetic field, while the channel $\alpha = 1$ is open only if $k_{Fn} \geq k^0_p + k^0_e$. The latter condition is opposite to the familiar condition $k_{Fn} \leq k_{Fp} + k_{Fe}$ in the field–free case. One has $\exp(-u_{s_n,\alpha}) \leq 1$ and $Q_\nu \propto b^2$, but one cannot expect Q_ν to be essentially larger than the field–free emissivity Q^0_ν as long as $B \lesssim 10^{19}$ G. Note also, that Eq. (25) describes the contribution of particles populating the ground Landau levels to the emissivity not only in the limit of superstrong fields. For it to be valid at moderate fields one should substitute number densities of e and p on the ground levels for n_e and n_p in the definition of $k^0_{e,p}$.

Similar result for the superstrong magnetic fields has been obtained recently by Leinson and Pérez (1997). Nevertheless, their expression differs from our in several respects. Most importantly, the authors got $(1+g_A^2)$ instead of $(1-g_A)^2$, which substantially overestimates the partial rate in the corresponding channel. Much more different result under the same assumptions was obtained by Bandyopadhyay et al. (1998). In our notations, the latter authors found the emissivity to be proportional to $\Theta(-u_{11})e^{-u_{11}}$, and obtained the spurious enhancement of the neutrino emission and additional acceleration of the cooling in a superstrong magnetic field. Their condition which opens the reaction channel is opposite to the actual one.

6. Conclusions

We have considered the neutrino emission produced by the direct Urca process in the cores of neutron stars with strong magnetic fields. We have derived the general expression for the neutrino emissivity [Eqs. (5) and (7)], and analysed it (Sect. 3) in the most important case, in which the magnetic field is not too strong, and the reacting electrons and protons populate many Landau levels. We have shown that the magnetic field can switch on the direct Urca process under the conditions, in which the field–free process is strongly suppressed by momentum conservation. We have obtained the analytical fit expressions (22) and (23) for this enhanced emissivity. We have performed a series of neutron star cooling simulations for the model, in which the star has a strong neutron superfluidity in the outer core but no superfluidity in the inner core. We have demonstrated, that the magnetic fields $B \lesssim 3 \cdot 10^{16}$ G in the stellar center can strongly enhance the neutrino luminosity and accelerate the cooling of neutron stars with masses by about 10% below the threshold mass, minimum mass of a star at which the field–free direct Urca process starts to be permitted. Therefore, the cooling can be controlled by the central stellar magnetic fields. The effect does not require superstrong fields $B \gtrsim 10^{18}$ G analysed by different authors.

Acknowledgements. D.A.B. is deeply thankful for hospitality at the Copernicus Astronomical center in Warsaw. This work was supported by RFBR (grant 96-02-16870a), RFBR-DFG (grant 96-02-00177G), INTAS (grant 96-0542), and KBN (grant 2 P03D 014 13).

References

Abramowitz M., Stegun I., 1970, Handbook of Mathematical Functions. Dover, New York

Bandyopadhyay D., Chakrabarty S., Dey P., Pal S., Rapid cooling of magnetized neutron stars. astro-ph/9804145

Baym G., Pethick C., Pines D., 1969, Nat 224, 673

Canuto V., Chiu H.Y., 1971, Space Sci. Rev. 12, 3

Dorofeev O.F., Rodionov V.N., Ternov I.M., 1985, Pisma Astron. Zh. 11, 302

Haensel P., Urpin V.A., Yakovlev D.G., 1990, A&A 229, 133

Kaminker A.D., Yakovlev D.G., 1981, Teoreticheskaya i matematicheskaya fizika.(Theoretical and mathematical physics), in Russian, 49, 248

Lai D., Shapiro S.L., 1991, ApJ 383, 745

Landau L.D., Lifshitz E.M., 1986, Statistical Physics Part I. Pergamon Press, Oxford

Lattimer J.M., Pethick C.J., Prakash M., Haensel P., 1991, Phys. Rev. Lett. 66, 2701

Leinson L.B., Pérez A., Direct Urca process in neutron stars with strong magnetic fields. astro-ph/9711216v2

Levenfish K.P., Yakovlev D.G., 1996, Astron. Lett. 22, 56

Meyer R.D., Pavlov G.G., Mészáros P., 1994, ApJ 433, 265

Østgaard E., Yakovlev D.G., 1992, Nucl. Phys., A540, 211

Page D., Applegate J.H., 1992, ApJ 394, L17

Pethick C.J., 1992, Rev. Mod. Phys. 64, 1133

Potekhin A.Y., Chabrier G., Yakovlev D.G., 1997, A&A 323, 415

Prakash M., Ainsworth T.L., Lattimer J.M., 1988, Phys. Rev. Lett. 61, 2518

Prakash M., Prakash M., Lattimer J.M., Pethick C.J., 1992, ApJ 390, L77

Takatsuka T., Tamagaki R., 1997, Prog. Theor. Phys. 97, 345

Wiringa R.B., Fiks V., Fabrocini A., 1988, Phys. Rev. C38, 1010

Yakovlev D.G., Kaminker A.D., Levenfish K.P., 1998, In: Shibazaki N., Kawai N., Shibata S., Kifune T. (eds.) Neutron Stars and Pulsars. Universal Acad. Press, Tokyo, p. 195